Progress In Electromagnetics Research, PIER 65, 71–80, 2006

MINIMIZING REFLECTION AND FOCUSSING OF INCIDENT WAVE TO ENHANCE ENERGY DEPOSITION IN PHOTODETECTOR'S ACTIVE REGION

A. A. Pavel, P. Kirawanich, and N. E. Islam

Department of Electrical and Computer Engineering
University of Missouri-Columbia
Columbia, MO 65211, USA

A. K. Sharma, C. S. Mayberry, and S. L. Lucero

Air Force Research Laboratory
Space Vehicles Directorate
Kirtland AFB, New Mexico 87117, USA

Abstract—Geometry of grating structure has been analyzed to maximize electromagnetic energy deposition onto the active region of a silicon photodetector. The concept of Brewster angle to minimize reflection from the grating surface and a differences-in-time technique to focus incoming electromagnetic radiation on the substrate has been applied to optimize the grated structure that amplifies transmitted energy through grating-substrate interface. The computed electric field at the interface for the new grating geometry has been found to be approximately 1.5 times higher than that of a square-shape gratings reported earlier. Also the average power depositions and electric field distributions on the grating-substrate interfaces have been studied which revealed the superiority of the proposed optimum structure.

1. INTRODUCTION

The compatibility of silicon (Si) with existing technology and the prospect of fabricating metal-semiconductor-metal (MSM) photodetectors at lower costs have generated renewed research interest in the analysis of such detectors. Enhancement of quantum efficiency of Si MSM detectors at relevant wavelengths by fabricating vertical and U-shaped trench electrodes [1], improvement of speed response through

fabrication of detectors on SOI substrate [2], use of hydrogenated amorphous Si (a-Si:H) for better absorption [3] have been reported. It was also shown that the collection efficiency of lateral MSM detectors can be improved with sub-micron wall-like gratings on the active detector region [4]. This improvement has been attributed to the enhanced deposition of electromagnetic energy at the grating-active region interface, primarily due to an increase in the transmitted energy as the plane wave travels from constricted grating region into comparatively larger cross sectional area of active region [5]. In this case, sudden change of structure dimensions at the interface provides a change in impedance to the plane wave and the reflection and transmission parameters are affected. Studies to enhance charge deposition through changes in the geometry, structure, and spacing of the gratings in the active region have been presented earlier [6].

In this paper we put forward the concept of further enhancing energy transmission into the active substrate through change in structural dimensions at the interface by designing optimum grating structure that would maximize the energy deposition onto the interface. Specifically reflection at the surface and focusing of EM energy as it travels through the grating structures into the substrate of the MSM detector has been optimized. Electromagnetic (EM) field transmission from air into surfaces with different geometry has been investigated for obtaining the grating structures that increase energy deposition onto the grating-substrate interface of a Si photodetector. The E-field amplitudes at the interface due to the previously reported and proposed grating structures have been compared to reveal their potentials. The electric field amplitude distribution along with average power deposition on the grating-substrate interfaces has also been investigated.

2. THEORIES TO ENHANCE ENERGY TRANSMISSION

The time averaged power transmitted $\langle P_t \rangle$ through the interface of any two different mediums is given by

$$\langle P_t \rangle = \langle P_i \rangle \cdot \frac{\eta_1}{\eta_2} \cdot |\tau|^2 = \langle P_i \rangle \cdot \frac{\eta_1}{\eta_2} \cdot \left(|1 - |r|^2\right) \cdot \frac{A_2}{A_1}, \tag{1}$$

where $\langle P_i \rangle$ is the average incident power to the interface, η_1 and η_2 are the intrinsic impedances of regions 1 and 2, respectively, r and τ are the reflection and transmission coefficients, respectively, and A_1 and A_2 are the cross sectional areas of regions 1 and 2, respectively. Fig. 1 shows the Si substrate with a square shape grating on top. For both Si-made gratings and substrate, η_1 is equal to η_2 and τ at the

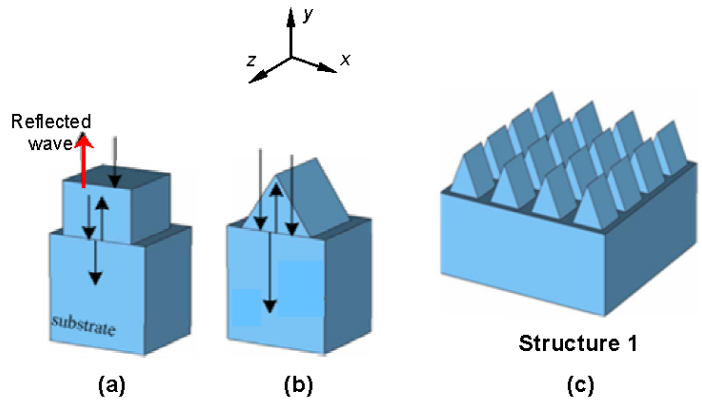

Figure 1. Cross sectional views of Si detectors with (a) square-shape grating [4] and (b) triangular-shape grating that exploits Brewster angle, showing reflection and transmission incident waves from various surfaces. (c) Arrangement of Structure 1-type gratings with Brewster angle on Si substrate used in simulations.

grating-substrate interface can be made greater than unity by ensuring that A_2 is larger than A_1 [5]. Higher value of τ means higher amount of power transmitted through the interface into the substrate active region.

However, the power transmission can be improved further by preventing the loss of energy due to the reflection of an incident plane wave from the top surface of the grating indicated by the arrows shown in Fig. 1(a). In order to prevent the loss from the top surface, we propose the grating structure with two inclined planes as shown in Fig. 1(b). This structure enhances $\langle P_i \rangle$ by exploiting the concept of Brewster's angle to prevent the reflection of an incoming x-polarized wave from the top surfaces of the grating. It is a well known phenomenon that for an incident plane wave with parallel or Transverse Magnetic (TM) polarization, there exists an incident angle for which the wave is totally transmitted into the second medium [7]. The angle is known as Brewster angle (θ_B) and is given by

$$\theta_B = \tan^{-1} \sqrt{\varepsilon_i / \varepsilon_t}, \tag{2}$$

where ε_i and ε_t represent the dielectric constants of the mediums containing the incident and reflected waves, respectively. To take advantage of this phenomenon, the inclined top surfaces of the grating were made to create an incident angle equal to θ_B with the incoming

plane wave with its E-field and H-field in $+z$ and $-x$ directions, respectively. Fig. 1(c) shows the associated structure used in the simulation and it is referred to as 'Structure 1' throughout the literature. With such a grating structure, nearly entire incident waves are expected to reach the grating-substrate interface and much higher amplitude of transmitted wave are likely to result. For silicon material, the incident angle is set to 78.83°.

Another mode of enhancing power deposition into the substrate is to focus the incoming radiation on to some spot on the interface. Such focusing is, however, certainly not achievable with a square shaped grating. This is simply because of significant differences in times taken by a wave to reach the expected focal point through different possible paths. The difference in the required times results in phase differences among the incoming EM waves that reach the point at a particular time through those paths. Such focusing can be achieved to some extent by a cone grating or a hatched-top cone-shaped grating that are referred as 'Structure 2' and 'Structure 3', respectively, as shown in Fig. 2. As will be demonstrated in detail elsewhere the differences in time (ΔT) taken by different possible paths of waves with that of straight-line one can be written in (3a) and (3b), respectively, for Structures 2 and 3 as

$$\Delta T(n) = \left\{\left(1 - \frac{n}{v_{norm}}\right) H - \sqrt{[n^2R^2 + (1-n)^2H^2]}\right\} \cdot v_{si}^{-1} \quad (3a)$$

$$\Delta T(n) = \left\{H^* - \sqrt{[n^2R^2 + (1-n)^2H^2]}\right\} \cdot v_{si}^{-1} \quad (3b)$$

where H and H^* are the heights of Structures 2 and 3, respectively, n is the ratio between the vertical distance of the wave entering point into the grating measured from the top to the full cone height, v_{norm} is the ratio between wave velocities in air to in silicon, R is the grating bottom radius, v_{si} is the wave velocity in silicon. By using Eqs. (3a) and (3b), it can be shown that for all n values, ΔT is smaller in case of Structure 3 implying that it should be more effective in depositing energy on the interface compared to that of Structure 2. Although Structures 2 and 3 are more effective to concentrate electromagnetic energy on the gratings-substrate interface compared to square-shape gratings, the value of ΔT taken by different paths can still be minimized. It can be shown that the points on the surface of a structure having distances x and y from the axis and top plane, respectively, should be given by the following relation in order to equalize the time required by EM waves

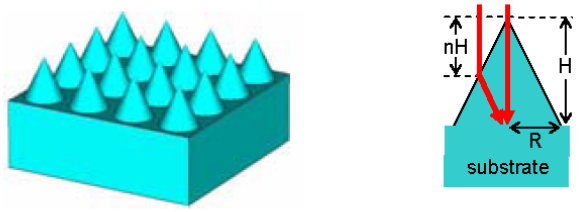

(a) Structure 2 (Cone)

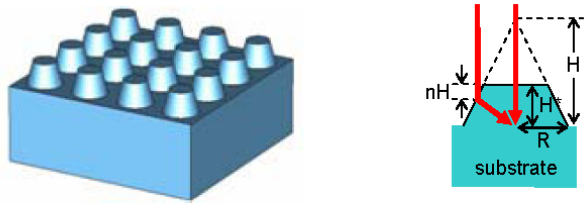

(b) Structure 3 (Hatched-top cone)

Figure 2. Some possible paths for electromagnetic wave to reach a focal point on grating-substrate interface for Structures 2 and 3 along with their arrangements on Si substrate used in simulations. The analysis the E-field intensity is based on the differences in time (ΔT) approach through Eqs. (3a) and (3b), respectively, for Structures 2 and 3.

to reach the focal point through any possible paths:

$$x(i) = \sqrt{\left[\left(H - \frac{y(i)}{v_{norm}}\right)^2 - (H - y(i))^2\right]}, \quad i = 1, 2, \ldots \tag{4}$$

The equation results in a relationship plot between the base and the height of the grating structure as shown in Fig. 3(a). The associated structure used in the simulation is shown in Fig. 3(b) and referred as 'Structure 4'. Certainly such a grating structure will be the most successful to focus the incoming radiation on the interface and hence to ensure maximum energy deposition into the substrates active region. Finally, one needs to evaluate and compare the average power depositions of different grating structures.

3. RESULTS AND DISCUSSIONS

Silicon substrates with four different grating structures discussed have been simulated to show the effects of the structures, geometries, and

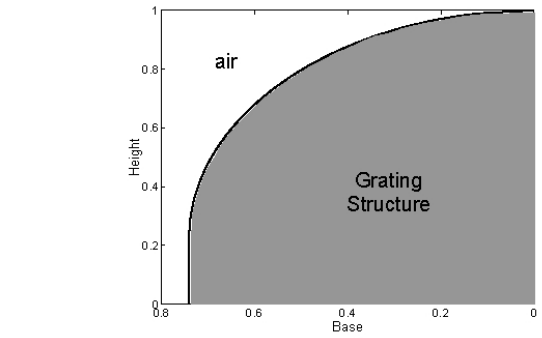

(a)

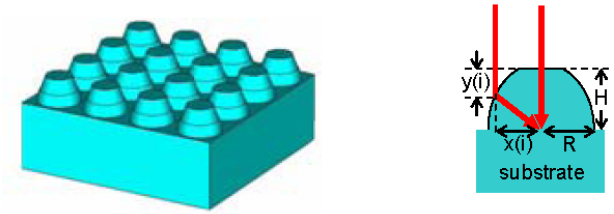

(b) Structure 4 (Optimum)

Figure 3. (a) Determination of optimum grating structure (Structure 4) with normalized dimension using Eq. (4). (b) Structure 4 used in the simulation.

shapes in enhancing the electromagnetic energy transmission into the substrate. Since the average power transmitted through the interface is proportional to the E-field magnitude at the interface, E-field probes were placed at the grating-substrate interface. Higher E-field amplitude at the interface indicates enhanced energy transmission into the active substrate that results in increased electron-hole pair generation or, in other words, increased charge collection efficiency of the detector. The simulation method has been based on Finite Integration Technique (FIT) providing discrete reformulation of Maxwell's equation in their integral form suitable for simulating electromagnetic field problems with complex geometries [5, 8]. For this purpose, a commercial code has been used that incorporates simulation equations using the mentioned technique [9]. A plane wave port with a continuous sinusoidal wave propagating in a normal direction to the xz plane has been used as a source of the excitation signal. The frequency of the excitation signal has been chosen to match the energy band gap

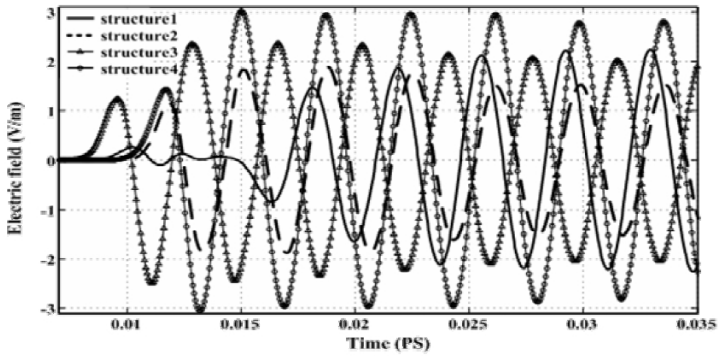

(a)

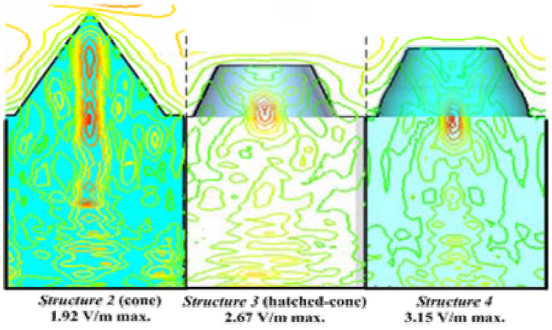

(b)

Figure 4. (a) Electric field amplitudes at interfaces of substrate in time domain as a function of grating structures presented in this paper. (b) Isoline plots of electric field and its maximum values for Structures 2, 3, and 4 and as to demonstrate focusing of incident EM radiation on interface. Noting that in Structure 4, the E-field is best concentrated on the surface.

of Si. All the four competing grating structure has been arranged in 4×4 form on $2\,\mu$m-thick (approximately $25\mu\text{m}^2$) Si substrates (see in Figs. 2 and 3). The height and dimension of the grating structures were varied to produce the optimum E-field intensity at the interface. The instantaneous E-field intensity measured by the probes at the various grating-substrate interfaces has been documented in Fig. 4(a) up to 0.035 ps as no significant change was observed after that. Moreover, it clearly points out the hierarchy of the grating structures in amplifying

E-field magnitude and Structure 4, as predicted, is recognized to be the best with maximum instantaneous field intensity more than 3 V/m. The maximum E-field magnitude at the interface of square-shaped gratings and substrate reported earlier was found to be approximately 1.5 V/m [5], which is less than that obtained with all four grating structures presented here. Fig. 4(b) demonstrates the maximum isoline plots of the incident wave transmitted through the gratings for Structures 2, 3, and 4 in to the substrates. This confirms the superiority of Structure 4 in concentrating electromagnetic radiation onto the interface. The maximum field strength with this grating structure was found to be 3.15 V/m, which is significantly larger than that found with square-shape or other grating structures presented here.

The distribution of electric field amplitudes in the xz plane of different structures are shown in Fig. 5 which reveals that electric field

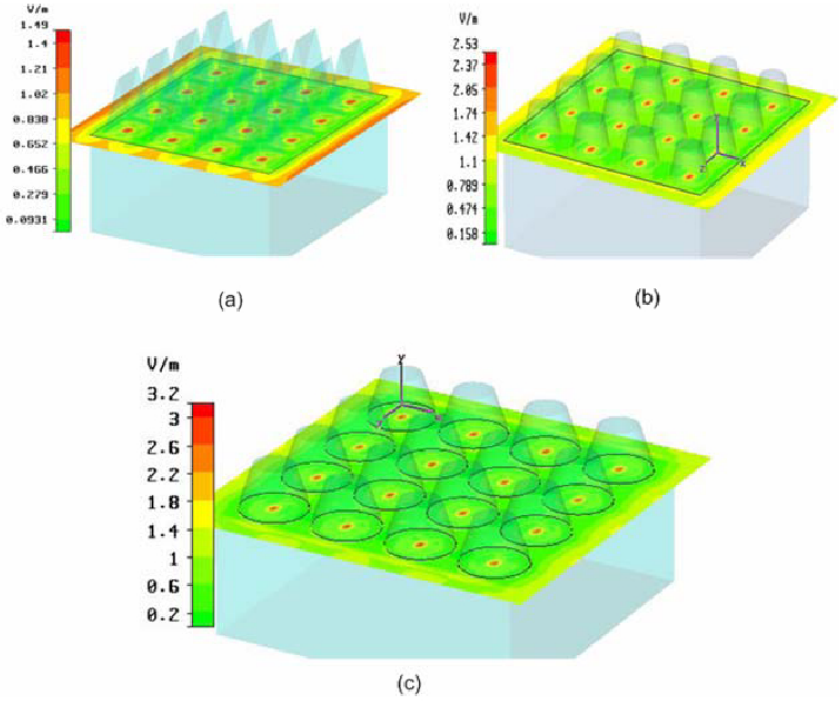

Figure 5. Electric field amplitude distribution in xz plane for (a) Structure 1 (b) Structure 3 and (c) Structure 4.

is rather concentrated at the mid-grating regions for all the structures discussed here. Since same numbers of different grating structures have been arranged on substrates with similar area, the average power deposition on the active substrate through grating structures can be assumed to be proportional to the measured E-fields. The amount of average energy deposition (P_t) by an electromagnetic wave transmitted to the active substrate-grating interface S is given by

$$P_t = \int_S \frac{1}{2} \frac{|E_t|^2}{\eta_S} \cdot ds \tag{5}$$

where E_t is the electric field amplitude transmitted to the substrate-grating interface and η_S is the intrinsic impedance of substrate. Taking the stable amplitude of the measured electric fields at grating-substrate interfaces of structures 2, 3 and 4, the average power deposition densities were found to be 7.5, 6.2 and 12.1 $\mathrm{mW/m^2}$, respectively, with an assumption that all structures have the same focusing surface areas (see Fig. 5). Structure 4 is therefore expected to deposit maximum energy on the active substrate due to enhanced focusing of electromagnetic field.

4. CONCLUSION

In this paper, different grating structures have been proposed and analyzed to increase the electromagnetic energy deposition on the active substrate surface of a Si MSM photodetector for enhancing its charge collection efficiency. It has been explained how energy deposition on the substrate surface can be increased by minimizing the difference among the time of travel requirements by different possible paths taken by waves to reach certain point at the interface. An optimum grating structure has been proposed based on this concept that results in producing an E-field amplitude that is almost twice as the one previously reported for square-shape grating at the interface. It is proposed that further investigation should be carried out to determine the optimum number of spikes of the grating structure (Structure 4) on a given surface area of Si substrate and the effect of doping density on the energy transmission through the grating.

REFERENCES

1. Ho, Y. L. and K. S. Wong, "Bandwidth enhancement in silicon metal-semiconductor-metal photodetector by trench formation," *IEEE Photon. Technol. Lett.,* Vol. 8, 1064–1066, 1996.

2. Liu, M. Y., E. Chen, and S. Y. Chou, "140-GHz metal-semiconductor-metal photodetectors on silicon-on-insulator substrate with a scaled active layer," *Appl. Phys. Lett.,* Vol. 65, 887–888, 1994.
3. Mott, N. F. and E. A. Davis, *Electronic Processes in Noncrystalline Materials,* 2nd ed., Oxford University Press, Oxford, U.K., 1979.
4. Sharma, A. K., S. H. Zaidi, P. C. Logofatu, and S. R. J. Brueck, "Optical and electrical proprties of nanostructured metal-semiconductor-metal photo detectors," *IEEE Journal of Quantum Electron.,* Vol. 38, 1651–1660, 2002.
5. Kranthi, N. S., M. O. Nizam, P. Kirawanich, N. E. Islam, A. K. Sharma, and S. L. Lucero, "Fields analysis of enhanced charge collection in nanoscale grated photo detectors," *Appl. Phys. Lett.,* Vol. 87, 244101, 2005.
6. Kache, S., N. S. Kranthi, M. O. Nizam, P. Kirawanich, R. W. McLaren, N. E. Islam, A. K. Sharma, C. S. Mayberry, and S. L. Lucero, "Field analysis to optimize charge collection in a sub-micron grated metal-semiconductor-metal photodetector," *Progress In Electromagnetics Research,* PIER 63, 75–88, 2006.
7. Kraus, J. D. and D. A. Fleisch, *Electromagnetics: With Applications,* 5th ed., WCB/McGraw-Hill, Boston, 1999.
8. Weiland, T., "A discretization method for the solution of Maxwell's equations for six-components fields," *Electrostatics and Communications,* Vol. 31, 116–120, 1977.
9. User Manual, CST Microwave Studio 5.0, Sonnet Software, Inc., 2005.